Electronic Supplementary Material (ESI) for Chemical Communications

Supporting Information

A Novel High-Spin Tridecanuclear Ni^{II} Cluster with an Azido-Bridged Core Exhibiting Disk-like Topology

Gabriel Brunet,[a] Fatemah Habib,[a] Cyril Cook,[a] Thushan Pathmalingam,[a] Francis Loiseau,[a] Ilia Korobkov,[a] Tara J. Burchell,[a] André Beauchemin,[a,b] Muralee Murugesu*[a,b]

[a] *Department of Chemistry, University of Ottawa, 10 Marie-Curie, Ottawa, ON, K1N6N5, Canada. Fax: (613) 562 5170; Tel : +1 613 562 5800-2733; E-mail: m.murugesu@uottawa.ca,*

[b] *Centre for Catalysis Research and Innovation, 30 Marie-Curie, Ottawa, ON, K1N6N5, Canada*

Experimental Section

Preparation of 1-(dimethylamino)propan-2-one oxime, Hdpo. A 100 mL round bottom flask equipped with a magnetic stir bar and a condenser was purged with argon. 3-(Dimethylamino)-1-propyne (30.0 mmol, 3.24 mL) and *n*-propanol (30 mL) were added to the flask followed by 50% wt aqueous hydroxylamine (45.1 mmol, 2.76 mL). The solution was refluxed under argon for 48 hours. After cooling the mixture to room temperature, the solvent was azeotroped with toluene (3 x 50 mL) and the mixture was recrystallized from MTBE (Methyl *tert*-Butyl Ether). The oxime was filtered and obtained as a pale yellow transparent crystal (2.47 g, 71%) mp 95.5-97.0 ^{o}C from MTBE; TLC R_f: 0.33 in 10% MeOH/CH_2Cl_2; ^{1}H NMR (300 MHz, DMSO-d_6) δ 10.48 (s, 1H), 2.83 (s, 2H), 2.09 (s, 6H), 1.75 (s, 3H); ^{13}C NMR (75 MHz, DMSO-d_6) δ 156.4, 63.6, 45.3, 12.3; IR (KBr pellet): 2964, 2877, 2839, 2724, 1853, 1657, 1470, 1279, 1258, 1181, 1041, 959, 933, 850, 674 cm^{-1}. HRMS (EI): Exact mass calculated for $C_5H_{11}NO$ [M]+: 116.0950, Found: 116.0941.

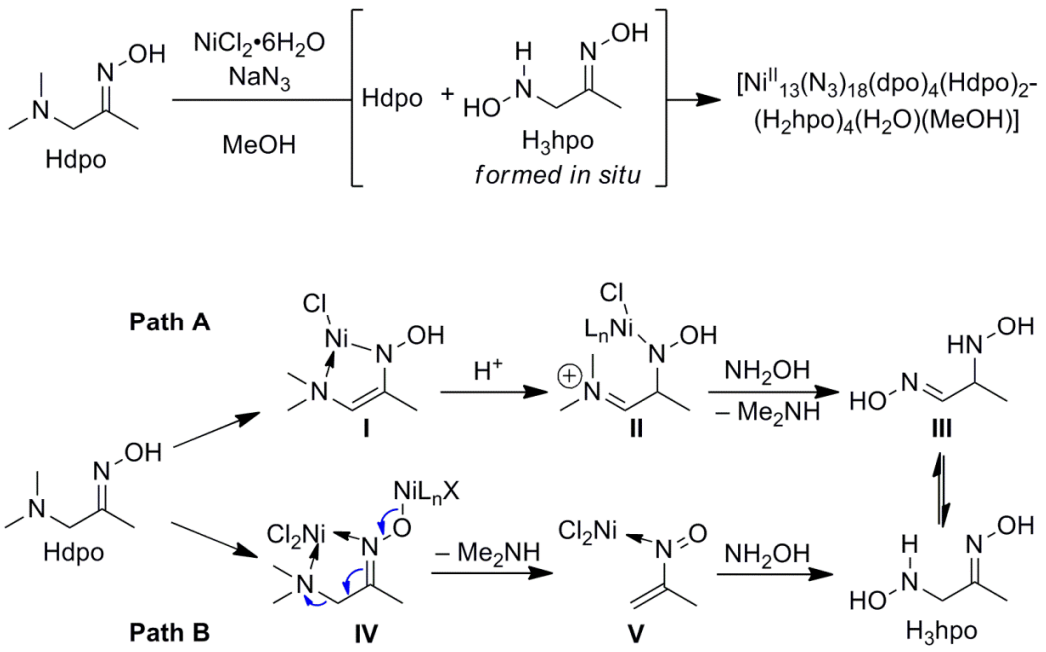

Scheme S1 Proposed mechanism for the partial conversion of Hdpo to H_3hpo.

Two pathways appear possible for conversion of Hdpo into H_3hpo in the conditions used for Ni^{II} cluster formation. Both involve an initially deprotonated intermediate and rely on partial oxime hydrolysis to generate free NH_2OH or an equivalent. In path A, **I** is formed from *α*-deprotonation of the activated Hdpo. Enamine protonation to **II** followed by condensation of NH_2OH provides aldoxime **III**, a tautomer of H_3hpo. In path B, base-catalyzed extrusion of Me_2NH on activated intermediate **IV** is followed by nucleophilic attack of NH_2OH to give H_3hpo.

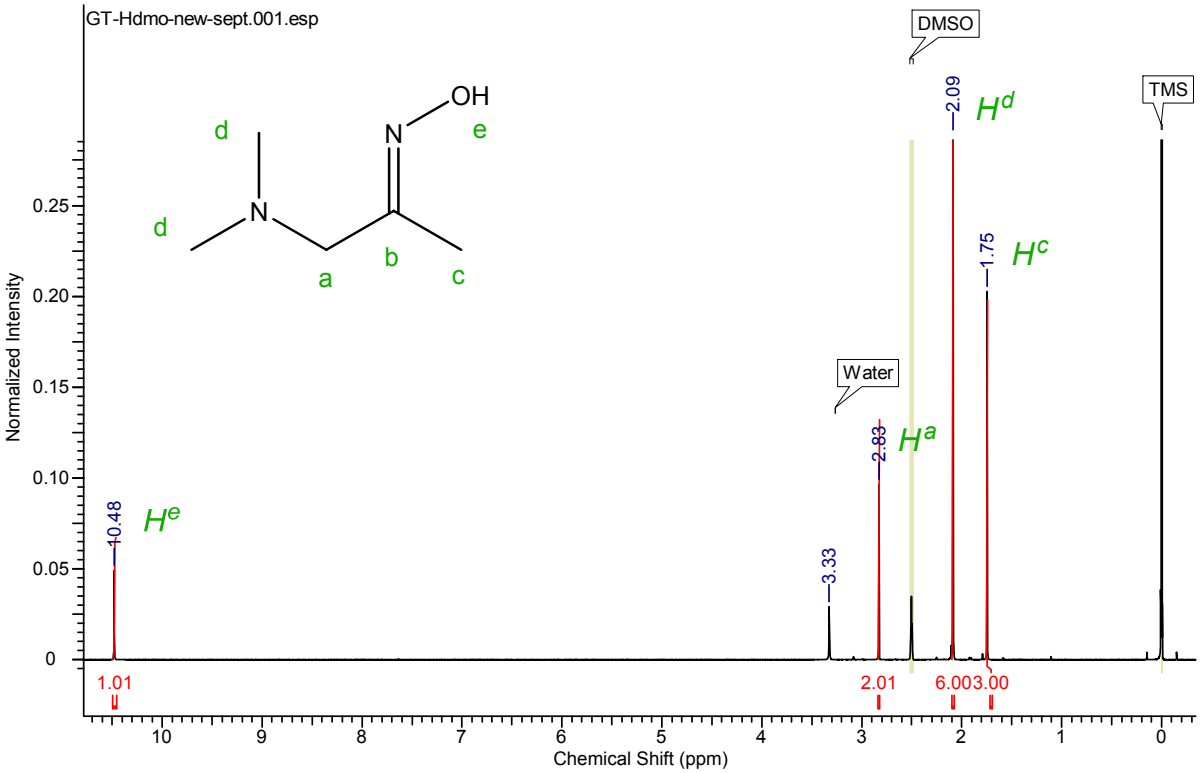

Fig. S1 H^1 NMR of Hdpo ligand.

Preparation of $[Ni^{II}_{13}(N_3)_{18}(dpo)_4(Hdpo)_2(H_2hpo)_4(H_2O)(MeOH)]$, 1. Complex **1** was synthesized by the reaction of $NiCl_2 \cdot 6H_2O$ (0.50 mmol, 118 mg) with Hdpo (0.50 mmol, 58 mg) and NaN_3 (1.0 mmol, 65 mg) in 20 mL of MeOH giving a clear green solution. Crystallization of the complex was achieved over a period of 5 days after which the solution was filtered to obtain dark-green hexagonal crystals in a yield ~ 5%. Selected IR (Nujol, cm^{-1}): 3430 (br), 2935 (s), 2931 (s), 2855 (s), 2112 (s), 2067 (s), 2046 (s), 1632 (m), 1500 (m), 1462 (s), 1377 (s), 1309 (m), 1241 (w), 1104 (w), 1075 (m), 1011 (w), 928 (w), 896 (w), 847 (m), 713 (w).

X-Ray crystallography

Crystals of **1** were grown from the mother liquor (MeOH solution) after 5 days. Compound **1** constantly produced only weakly diffracting crystals therefore presented results is the best out of series of data collection attempts. The crystal of **1** was mounted on thin glass fibre using paraffin oil and sample was cooled to 200 °K prior to data collection. Data were collected on a Bruker AXS SMART single crystal diffractometer equipped with a sealed Mo tube source (wavelength 0.71073 Å) APEX II CCD detector. Raw data collection and processing were performed with APEX II software package from BRUKER AXS.[1] Diffraction data for **1** sample were collected with a sequence of 0.5° ω scans at 0, 90, 180, and 270° in φ. Initial unit cell parameters were determined from 60 data frames collected at the different sections of the Ewald sphere. Collection of data was carried out up to Å, 0.75 Å (28.27° in Q). However it was discovered based on R(int) and R(s) values that no useful structural data can be found past 0.95 Å (22.08 ° in Q) resolution with both R(int) and R(s) exceeding 50%. Based on these values data set was trimmed and only data above 0.95 Å were used for structure solution and refinement. Semi-empirical absorption corrections based on equivalent reflections were applied.[2] Systematic absences in the diffraction data-set and unit-cell parameters were consistent with monoclinic $P2_1$ (№4) space group. Solutions in non-centrosymmetric space group yielded chemically reasonable and computationally stable results of refinement. However, in order to obtain reasonable thermal parameters and preserve reasonable data to parameters ratio “thermal motion” and “rigid bond” restrains were applied to all non-hydrogen atoms. The structure was solved by direct methods, completed with difference Fourier synthesis, and refined with full-matrix least-squares procedures based on F^2. In the structure compound molecules are situated in the general position. All non-hydrogen atoms were refined anisotropically with satisfactory thermal parameters values. Results of refinement suggested the presence of inversion twinning. Twinning parameter for inversion twinning was refined as 27%. Positions of all hydrogen atoms were generated based on molecular geometry and all hydrogen atoms were treated as idealized contributions. All scattering factors are contained in several versions of the SHELXTL program library, with the latest version used being v.6.12[3] Crystallographic data and selected data collection parameters are reported in Tables S1.

1. APEX Software Suite v.2010; Bruker AXS: Madison, WI, 2005.
2. R. Blessing, *Acta Cryst.* 1995, **A51**, 33.
3. G. M. Sheldrick, *Cell Now*, 2004**,** Bruker-AXS, Inc., Madison, WI

Magnetic measurements

The magnetic susceptibility measurements were performed using a Quantum Design SQUID magnetometer MPMS-XL that operates between 1.8 and 300 K for dc applied fields ranging from -7 to 7 T. Measurements were performed on 15.4 mg of ground polycrystalline sample. The magnetic data were corrected for the sample holder as well as the diamagnetic contribution. Additionally, the sample was checked for the presence of ferromagnetic impurities by measuring the magnetization as a function of the field at 100 K. For pure paramagnetic or diamagnetic systems, a perfect straight line is expected and is indeed observed for this compound, indicating the absence of any ferromagnetic impurities.

Table S1. Crystallographic data and selected data collection parameters for **1**.

Compound	mm094
Empirical formula	$Ni_{26}C_{85}H_{190}N_{148}O_{34}$
Formula weight	5356.31
Crystal size, mm	0.26 x 0.18 x 0.17
Crystal system	Monoclinic
Space group	$P2_1$ №4
Z	2
a, Å	19.046(3)
b, Å	29.147(6)
c, Å	23.518(4)
α, °	90
β, °	100.477(11)
γ, °	90
Volume, $Å^3$	12838(4)
Calculated density, Mg/m^3	1.386
Absorption coefficient, mm^{-1}	1.931
F(000)	5472
Θ range for data collection, °	1.67 to 27.75 (trimmed to 1.67 to 21.97)
Limiting indices	h = ±20,-26 <= k< = +30, l = ±24
Reflections collected / unique	78643 / 26123
R(int)	0.0841
Completeness to Θ = 28.34, %	99.3
Max. and min. transmission	0.7349 and 0.6337
Data / restraints / parameters	26123 / 2439 / 2639
Goodness-of-fit on F^2	1.041
Final R indices [I>2σ(I)]	R_1 = 0.0763, wR_2 = 0.1922
R indices (all data)	R_1 = 0.1334, wR_2 = 0.2366
Largest diff. peak/hole, $e·Å^{-3}$	0.952 and -1.023
Absolute structure parameter	0.27(3)

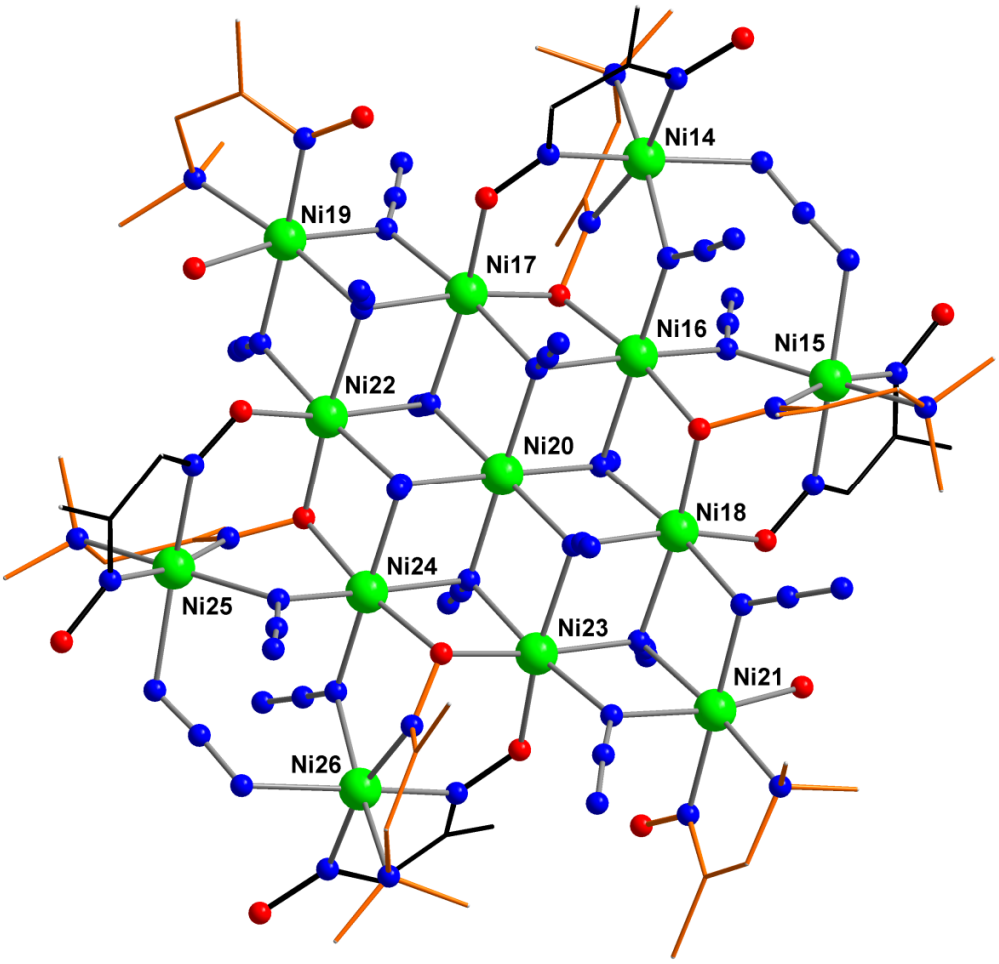

Fig. S2 Partially labeled tridecanuclear structure of complex **1B**. Hdpo and dpo^{-} ligands are shown in orange while H_2hpo ligands are shown in black. Color code: Green (Ni^{II}), blue (N), red (O).

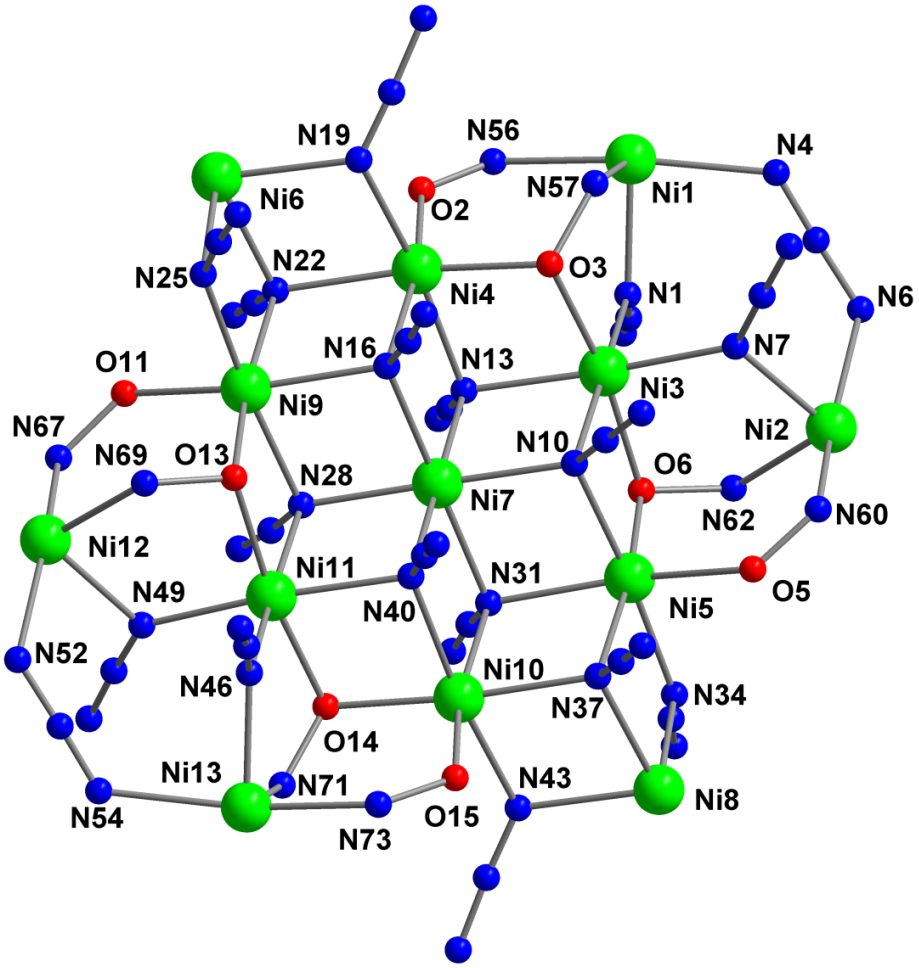

Fig. S3 Fully labeled core structure of **1A**.

Table S2. Selected bond distances (Å), angles (°) and torsion angles (°) for complex **1A**.

Bond distances (Å)							
Ni(7)-Ni(4)	3.234(3)	Ni(4)-N(19)	2.15(1)	Ni(9)-N(16)	2.17(1)	Ni(1)-N(1)	2.03(2)
Ni(7)-Ni(3)	3.141(3)	Ni(5)-O(5)	2.15(2)	Ni(9)-N(28)	2.14(1)	Ni(1)-N(57)	2.03(2)
Ni(7)-Ni(5)	3.165(3)	Ni(5)-O(6)	2.04(1)	Ni(10)-N(37)	2.12(1)	Ni(1)-N(56)	2.11(2)
Ni(7)-Ni(10)	3.241(3)	Ni(5)-N(10)	2.04(1)	Ni(10)-N(43)	2.12(1)	Ni(2)-N(6)	2.22(2)
Ni(7)-Ni(11)	3.139(3)	Ni(5)-N(31)	2.08(1)	Ni(10)-O(15)	2.13(2)	Ni(2)-N(7)	2.09(2)
Ni(7)-Ni(9)	3.163(3)	Ni(5)-N(37)	2.16(1)	Ni(10)-O(14)	2.04(1)	Ni(2)-N(62)	2.02(2)
Ni(4)-Ni(6)	3.276(3)	Ni(5)-N(34)	2.19(1)	Ni(10)-N(40)	2.05(1)	Ni(2)-N(60)	2.03(2)
Ni(4)-Ni(9)	3.255(3)	Ni(6)-N(19)	2.07(2)	Ni(10)-N(31)	2.12(1)	Ni(3)- N(1)	2.07(2)
Ni(4)-Ni(3)	3.150(3)	Ni(6)-N(22)	2.18(2)	Ni(11)-N(28)	2.17(1)	Ni(3)-N(7)	2.09(2)
Ni(4)-Ni(1)	3.918(3)	Ni(6)-N(25)	2.12(2)	Ni(11)-N(40)	2.13(1)	Ni(3)-O(6)	2.04(1)
Ni(3)-Ni(1)	3.400(3)	Ni(7)-N(13)	2.12(2)	Ni(11)-O(14)	2.07(1)	Ni(3)-N(10)	2.15(1)
Ni(3)-Ni(2)	3.441(3)	Ni(7)-N(10)	2.11(1)	Ni(11)-N(46)	2.09(2)	Ni(3)-N(13)	2.12(1)
Ni(3)-Ni(5)	3.138(3)	Ni(7)-N(31)	2.09(1)	Ni(11)-N(49)	2.08(2)	Ni(3)-O(3)	2.06(1)
Ni(5)-Ni(2)	3.803(3)	Ni(7)-N(40)	2.12(1)	Ni(11)-O(13)	2.03(1)	Ni(4)-O(2)	2.03(1)
Ni(5)-Ni(8)	3.193(3)	Ni(7)-N(28)	2.13(1)	Ni(12)-N(67)	2.06(2)	Ni(4)-O(3)	2.04(1)
Ni(5)-Ni(10)	3.247(3)	Ni(7)-N(16)	2.09(1)	Ni(12)-N(69)	2.01(2)	Ni(13)-N(54)	2.19(1)
Ni(10)-Ni(8)	3.268(3)	Ni(8)-N(34)	2.09(1)	Ni(12)-N(49)	2.13(1)	Ni(13)-N(46)	2.02(2)
Ni(10)-Ni(11)	3.154(3)	Ni(8)-N(37)	2.08(2)	Ni(12)-N(52)	2.19(2)	Ni(13)-N(71)	2.02(2)
Ni(10)-Ni(13)	3.914(3)	Ni(8)-N(43)	2.15(1)	Ni(11)-Ni(12)	3.421(3)	Ni(13)-N(73)	2.04(1)
Ni(11)-Ni(13)	3.401(3)	Ni(9)-O(13)	2.15(1)	Ni(11)-Ni(9)	3.143(3)	Ni(4)-N(22)	2.18(1)
Ni(4)-N(13)	2.04(1)	Ni(9)-O(11)	2.04(1)	Ni(9)-Ni(12)	3.793(3)	Ni(9)-N(22)	2.05(2)
Ni(4)-N(16)	2.11(1)	Ni(9)-N(25)	2.02(1)	Ni(9)-Ni(6)	3.181(3)	Ni(1)-N(4)	2.15(1)
Bond angles (°)							
Ni(3)-N(7)-Ni(2)	110.86	Ni(4)-N(16)-Ni(7)	39.71	Ni(11)-O(13)-N(69)	110.44	Ni(1)-N(4)-Ni(5)	123.65
Ni(3)-O(6)-N(62)	111.96	Ni(4)-N(13)-Ni(7)	100.15	Ni(11)-N(49)-Ni(12)	108.75	Ni(5)-O(5)-N(60)	126.76
Ni(3)-N(1)-Ni(1)	111.82	Ni(4)-O(3)-N(57)	112.17	Ni(11)-N(46)-Ni(13)	111.91	Ni(5)-N(34)-Ni(8)	100.48
Ni(3)-O(3)-Ni(4)	100.40	Ni(9)-N(22)-Ni(6)	95.85	Ni(11)-O(14)-N(71)	108.82	Ni(5)-N(37)-Ni(8)	94.66
Ni(3)-O(3)-N(57)	107.65	Ni(9)-N(25)-Ni(6)	99.44	Ni(11)-O(14)-Ni(10)	39.78	Ni(5)-N(31)-Ni(7)	95.43
Ni(3)-N(13)-Ni(4)	96.32	Ni(9)-N(16)-Ni(7)	96.72	Ni(11)-N(40)-Ni(7)	95.08	Ni(5)-N(10)-Ni(7)	98.67
Ni(3)-N(13)-Ni(7)	95.82	Ni(10)-N(31)-Ni(5)	41.30	Ni(11)-N(40)-Ni(10)	41.98	Ni(5)-O(6)-N(62)	110.36
Ni(3)-N(10)-Ni(7)	63.51	Ni(10)-N(37)-Ni(5)	97.65	Ni(12)-N(52)-N(53)	121.51	Ni(13)-N(73)-O(15)	127.84
Ni(3)-N(10)-Ni(5)	57.18	Ni(10)-N(37)-Ni(8)	40.34	Ni(12)-N(67)-O(11)	124.98	Ni(13)-N(71)-O(14)	123.24
Ni(3)-O(6)-Ni(5)	100.50	Ni(10)-N(31)-Ni(7)	98.24	Ni(12)-N(69)-O(13)	121.71	Ni(13)-N(54)-N(53)	125.18
Ni(4)-O(2)-N(56)	129.16	Ni(10)-N(43)-Ni(8)	99.44	Ni(2)-N(5)-N(5)	116.79	Ni(9)-O(11)-N(67)	126.22
Ni(4)-N(19)-Ni(6)	98.50	Ni(10)-O(15)-Ni(73)	127.19	Ni(2)-N(62)-O(6)	120.18	Ni(9)-O(13)-N(69)	111.60
Ni(4)-N(22)-Ni(6)	100.22	Ni(10)-O(14)-Ni(71)	113.52	Ni(2)-N(60)-O(5)	127.25	Ni(9)-O(13)-Ni(11)	39.43
Ni(4)-N(22)-Ni(9)	41.21	Ni(10)-N(40)-Ni(7)	99.31	Ni(1)-N(57)-O(3)	123.60	Ni(9)-N(28)-Ni(11)	95.41
Ni(4)-N(16)-Ni(9)	97.63	Ni(11)-N(28)-Ni(7)	96.20	Ni(1)-N(56)-O(2)	127.42	Ni(9)-N(28)-Ni(7)	40.79
Torsion angles (°)							
Ni(1)-N(57)-O(3)-Ni(4)	71.01	Ni(2)-N(62)-O(6)-Ni(5)	16.13	Ni(12)-N(69)-O(13)-Ni(9)	39.04		
Ni(1)-N(57)-O(3)-Ni(3)	25.54	Ni(2)-N(62)-O(6)-Ni(5)	39.95	Ni(13)-N(71)-O(14)-Ni(11)	39.24		
Ni(1)-N(60)-O(5)-Ni(5)	16.13	Ni(12)-N(69)-O(13)-Ni(11)	42.64	Ni(13)-N(71)-O(14)-Ni(10)	71.24		
Ni(1)-N(56)-O(2)-Ni(4)	17.13	Ni(12)-N(67)-O(11)-Ni(9)	21.90	Ni(13)-N(73)-O(15)-Ni(10)	20.78		
Ni(2)-N(62)-O(6)-Ni(3)	40.19						

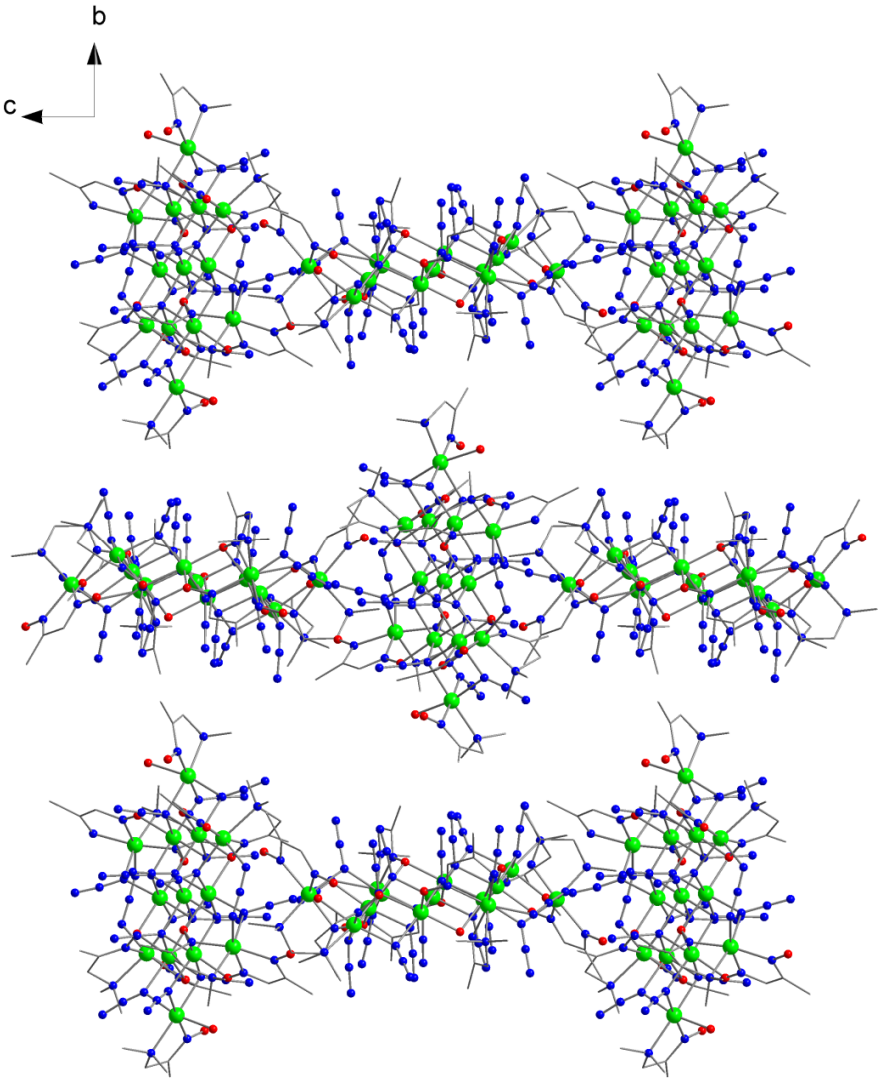

Fig. S4 Packing arrangement of **1** along the *a*-axis.

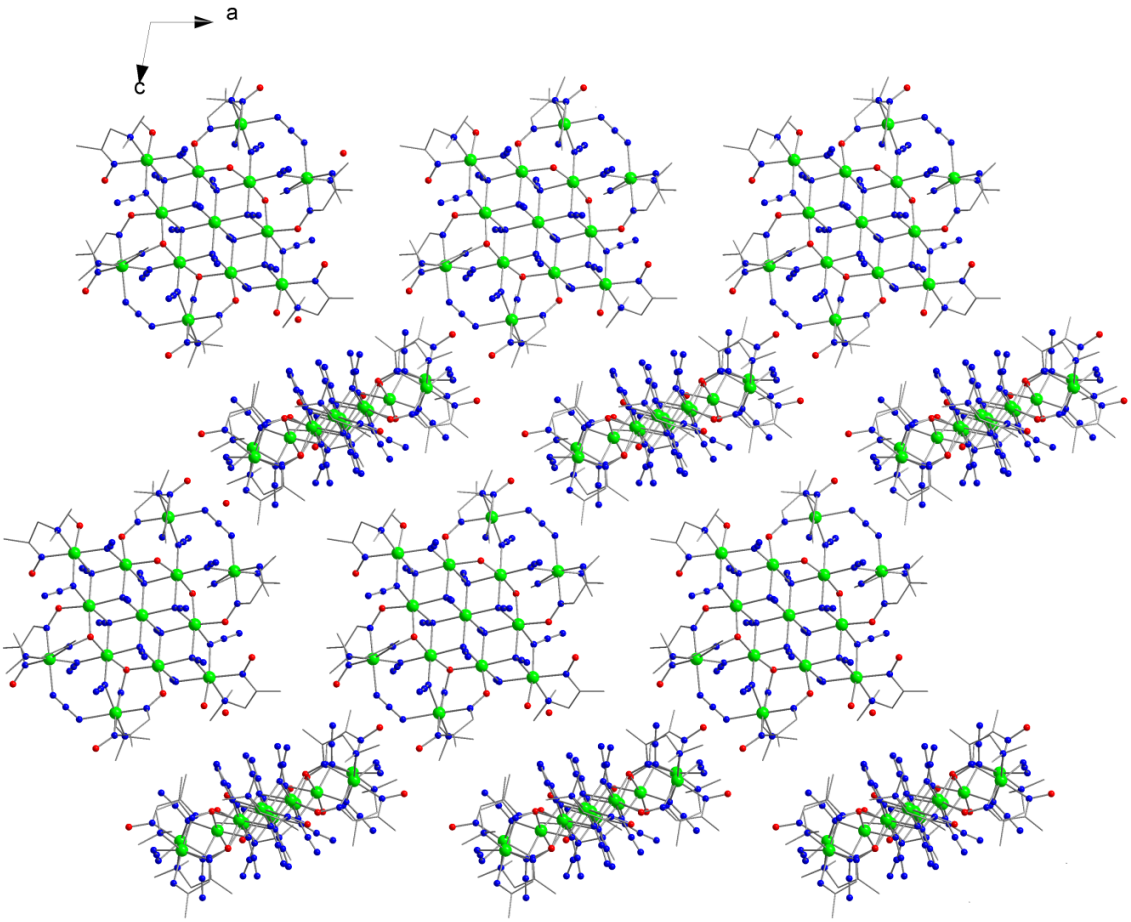

Fig. S5 Packing arrangement of **1** along the *b*-axis.

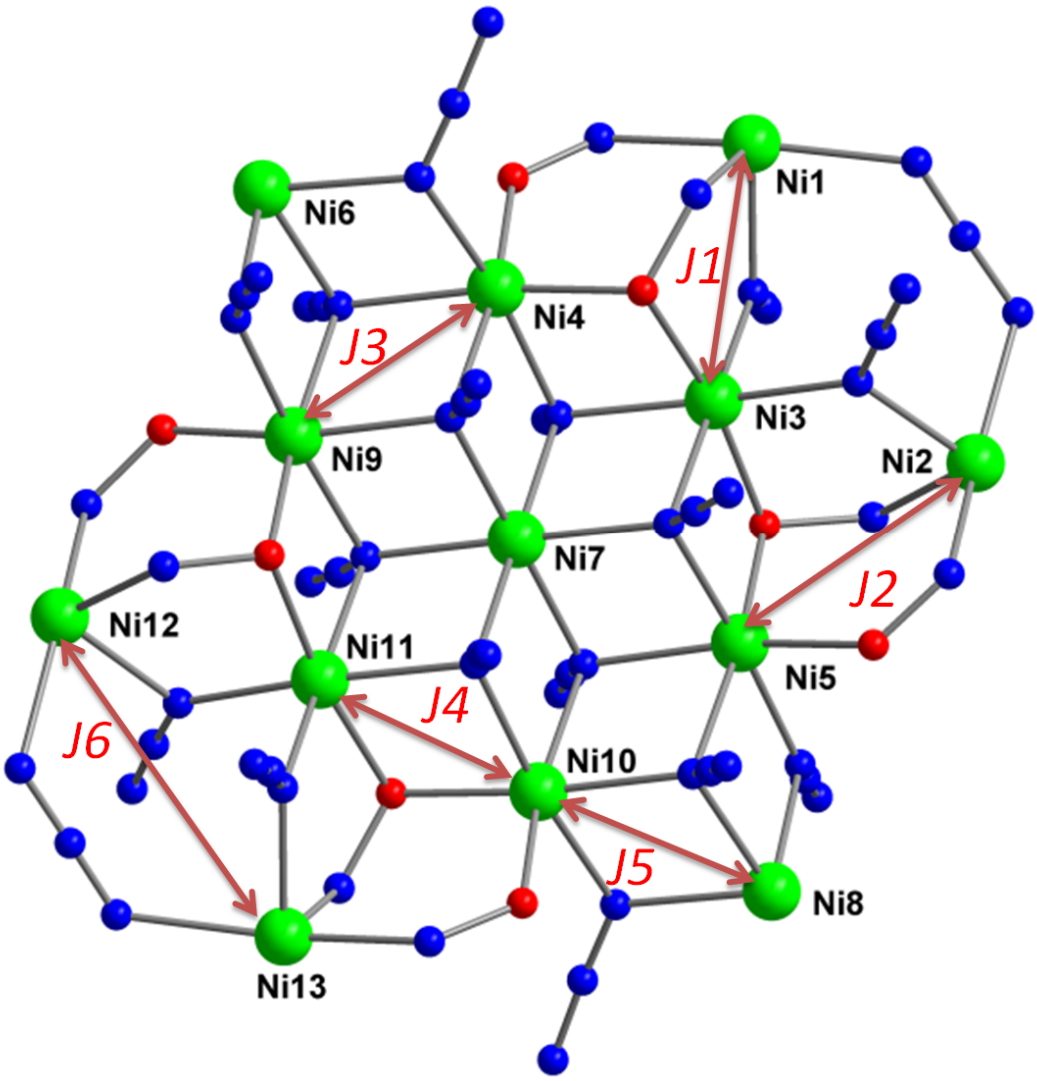

Fig. S6 Core structure of **1** showing six different magnetic superexchange pathways, *J1*-*J6*.

Electronic Supplementary Material (ESI) for Chemical Communications

TOC Picture